# Engineering Notes

## Verification and Validation Framework for Autonomous Rendezvous Systems in Terminal Phase

Wenfei Wang,* Prathyush Menon,† and Declan Bates‡
*University of Exeter, Exeter EX4 4QF, United Kingdom*
Simone Ciabuschi,§ Nuno M. Gomes Paulino,§ and Emanuele Di Sotto¶
*GMV Aerospace, 28760 Madrid, Spain*
Ambroise Bidaux** and Aymeric Kron††
*NGC Aerospace, Ltd., Sherbrooke, Quebec J1J 2C3, Canada*
and
Sohrab Salehi‡‡ and Samir Bennani§§
*ESA, Noordwijk, The Netherlands*

DOI: 10.2514/1.A32531



### I. Introduction

THIS Note reports results from a study carried out for the ESA with the objective of improving the safety of future autonomous rendezvous guidance, navigation, and control (GNC) systems during the terminal rendezvous mission phase, recognized as a key capability for Mars sample return (MSR). The robustness of the critical terminal phase of the mission must be rigorously investigated under different conditions [1,2]. Availability of reliable verification and validation (VV) techniques, which can estimate the worst-case behavior of the system to provide guarantees of correct functionality with a desired safety level under different mission scenarios with a large number of uncertain conditions [3], is key to the success of the mission. In the case of collision avoidance, for example, the distance between chaser and target must be proven to always be greater than a specified minimum value even under worst-case conditions during the approach phase [1,4]. The most widely used VV technique in the space industry is still Monte Carlo (MC) simulation campaigns, which randomly explore the uncertain parameter space using high-performance simulators. Although easy to implement, key drawbacks are computational complexity and lack of guarantee to assess the true worst-case (rare event) behavior of the system; see the results in [5] for an example of this phenomenon in the context of reusable launch vehicles.

The contribution of the Note is an integrated approach combining the analytical $\mu$ analysis and the simulation-and-optimization-based method [5], which includes the global optimization algorithms such as Differential Evolution (DE) and Dividing Rectangles (DIRECT), as well as local optimization algorithm Nealder–Mead simplex [6]. The worst-case behavior of an autonomous rendezvous system, based on the industry standard high-integrity autonomous rendezvous and docking (HARVD) and GNC system [7] during the terminal rendezvous phase of a realistic MSR mission scenario, obtained by the proposed approach reveals the significant potential of the methodology when compared with traditional Monte Carlo simulations, in terms of both reliability and efficiency.

### II. Autonomous Rendezvous System and Evaluation Criterion

The scenario considered in this study using a tailored HARVD functional engineering simulator for the MSR mission concerns only the terminal phase using the GNC system in which a chaser (1575 kg) approaches the target from 3000 m range up to the capture point using relative measurements from short-range sensors [7]. The resulting nominal timeline for the terminal rendezvous phase consists of V-bar hops, V-bar forced translation, and free drift until capture. In V-bar hops, the chaser executes five hops and six station-keeping positions including starting and final points (−3000, −1600, −800, −400, −200, 100 m); see top subfigure of Fig. 1. In V-bar forced translation, the chaser decreases its velocity as it approaches the target as shown in the lower subfigure of Fig. 1. Further details about these maneuvers can be found in [1]. Additional details on the models of spacecraft, sensor, and actuators in HARVD simulator can be found in [7].

#### A. Guidance, Navigation, and Control Requirements and Evaluation Metrics

The baseline requirements for the successful capture to be obtained by the GNC, based on the MSR mission capture conditions, are defined as lateral position misalignment ($Xl_f$ with nominal value 0.0 m and maximum variation 0.20 m), lateral velocity error ($Vl_f$ with nominal value 0.0 m/s and maximum variation 0.04 m/s), and the longitudinal velocity error ($V\text{lon}_f$ with nominal value 0.1 m/s and maximum variation 0.05 m/s). The evaluation criterion used for this analysis is given as

$$FoM = w_1 E(Xl_f) + w_2 E(Vl_f) + w_3 E(V\text{lon}_f) \tag{1}$$

where $E(\cdot)$ is the percentage error with respect to the difference between the maximum allowed variation and the nominal value for the considered variable (lateral position, lateral velocity, and longitudinal velocity, respectively) at the capture conditions. The term $w_i$ represents the weight given to each condition in the criterion, such that $w_1 + w_2 + w_3 = 1$. The terms in Eq. (1) are as follows:

$$E(Xl_f) = \left| \frac{Xl_f - Xl_{f\text{nom}}}{Xl_{f\,\max} - Xl_{f\text{nom}}} \right|, \quad E(Vl_f) = \left| \frac{Vl_f - Vl_{f\text{nom}}}{Vl_{f\,\max} - Vl_{f\text{nom}}} \right|,$$
$$E(V\text{lon}_f) = \left| \frac{V\text{lon}_f - V\text{lon}_{f\text{nom}}}{V\text{lon}_{f\,\max} - V\text{lon}_{f\text{nom}}} \right| \tag{2}$$

Presented as Paper 2012-4925 at the AIAA Guidance, Navigation, and Control Conference, Minneapolis, MN, 13–16 August 2012; received 29 October 2012; revision received 8 July 2014; accepted for publication 10 July 2014; published online 15 October 2014. 

*Associate Research Fellow, College of Engineering, Mathematics and Physical Sciences, Harrison Building, North Park Road.
†Lecturer, College of Engineering, Mathematics and Physical Sciences, Harrison Building, North Park Road.
‡Professor, College of Engineering, Mathematics and Physical Sciences, Harrison Building, North Park Road.
§Project Engineer, Isaac Newton, 11 Parque Tecnologico Madrid Tres Cantos.
¶Project Manager, Isaac Newton, 11 Parque Tecnologico Madrid Tres Cantos.
**Project Engineer, 1650 rue King Quest Bureau 202.
††Project Manager, 1650 rue King Quest Bureau 202.
‡‡Guidance, Navigation, and Control System Engineer, Rhea System, European Space Research and Technology Centre, Postbus 299, 2200 AG.
§§Guidance, Navigation, and Control System Engineer, European Space Research and Technology Centre, TEC-ECN, Keplerlaan 1, 2201 AZ.

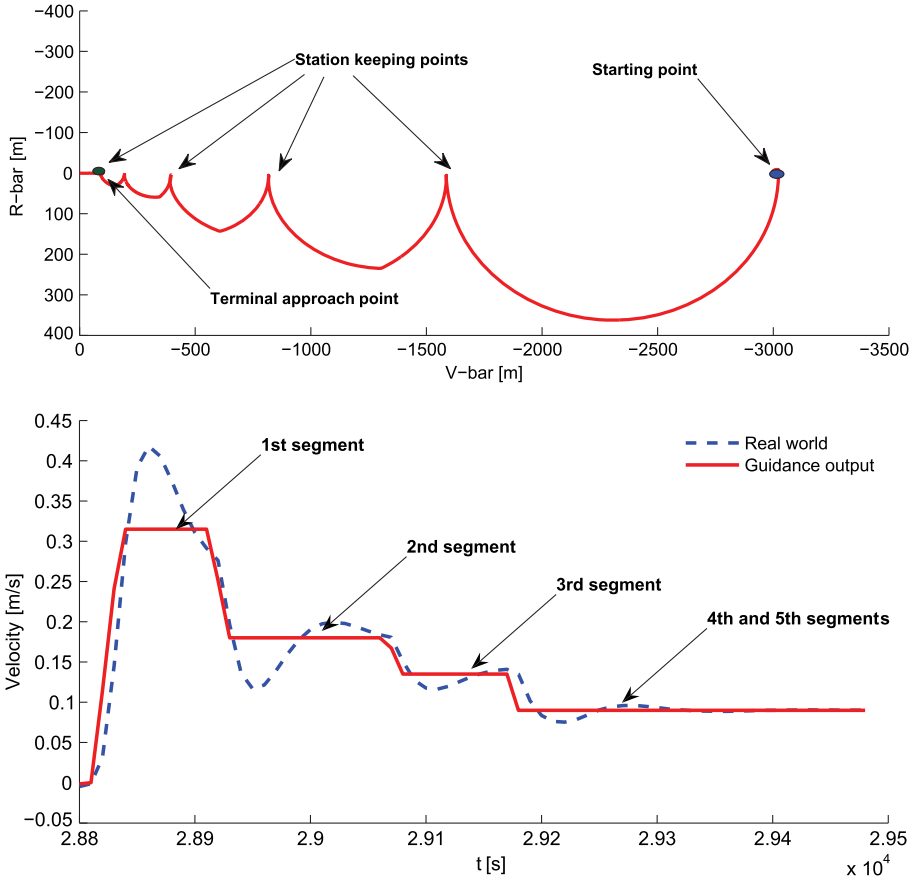


**Fig. 1 Relative path for the terminal phase and decreasing approach velocities during the forced motion phase.**



where $(\cdot)_{f\text{nom}}$ and $(\cdot)_{f\,\max}$ are the corresponding nominal and maximum allowed values at the capture. The worst case maximizes the figure of merit in Eq. (1), with each $w_i = 1/3$.

### B. Uncertain Parameters Considered for Verification and Validation

Two categories of uncertain parameters with a uniform distribution are considered. The first is the design uncertainties set (DUS), which represents the 49 uncertain parameters considered during the control system design phase. The DUS consists of the chaser initial relative position and velocity (6), absolute knowledge of target initial state (6), chaser's mass (1), inertia (9), center of mass (1), Lidar misalignment (2), thrust magnitude bias (8), and thrust misalignment (16), so that the total of the numbers in parentheses adds up to 49. The second is the enhanced uncertainties set (EUS), comprised of 118 uncertainties, including the thruster's location (24), gyroscope misalignment (3), bias (6) and scale factors (6), star tracker's misalignment (6), reaction wheels misalignment (8) and chaser flexible modes such as the solar array's frequencies (8) and damping factors (8), and entire DUS (49). This set of uncertainties, in which additional uncertain parameters are included, particularly those related to the active sensors and actuators, is considered in order to check the VV performance beyond the initial design specification. Thus, the EUS contains additional uncertainties that are not considered during the design phase.

## III. Integrated Verification and Validation Framework

The proposed strategy steers the optimization-based analysis, in terms of both the starting point and the search region, by means of $\mu$ analysis results, with the expectation that this will allow faster convergence in the search for problematic cases. In particular, the optimization algorithm is initialized at the worst-case parameter combination derived from the peak of the $\mu$ lower bound, while the uncertain parameter search space is reduced to the area where the parameters are beyond the limit of guaranteed robustness that the $\mu$ analysis has identified. Algorithm 1 encapsulates the steps involved in the proposed integrated analysis. In addition, the process to compute a reduced region and the probabilities associated with finding a violation case in a subregion based on the sensitivity are provided in [8]. For the problem defined in this Note, some of the uncertainties, such as the variation of the initial states of the chaser spacecraft, cannot be taken into account during the linear fractional transformation (LFT) modeling and hence in the subsequent $\mu$ analysis [9]. This restriction does not apply to the optimization-based approach, which can deal with any type of uncertainty in the simulator.

Based on this fact, denoting the uncertain parameters considered by LFT/$\mu$ as set $S_1$ and the remaining uncertainties as set $S_2$, we attempted to integrate both methods in two different ways:

1) For the uncertain parameters in set $S_1$, optimization methods were driven by the redefined bounds and initial values derived from LFT/$\mu$, while the other parameters in set $S_2$ were treated as per the original settings.

2) Uncertain parameters in set $S_1$ were considered as known parameters with values fixed in the worst cases identified by LFT/$\mu$. Only the uncertain parameters in set $S_2$ were then taken into account by the optimization algorithms. Note that in this approach the dimension of the search space for the optimization algorithms was significantly reduced. The $\mu$ analysis computation can be time consuming in certain cases, particularly when linear-matrix-inequality-based analysis is required on a large LFT. However, the $\mu$ analysis had fast convergence in all the studies reported in this Note and was completed in couple of minutes, which is significantly faster than the time domain simulation.

## IV. Worst-Case Analysis Results

Validation results from a simplified rendezvous scenario are reported in [10]. Here, the integrated analytical and optimization approaches given in Algorithm 1 are applied sequentially to validate

**Algorithm 1 Integrated VV framework**

1. Define the uncertain set $S$ for the simulator and $S_1$ for the LFT model, where $S_1 \cup S_2 = S$. The variation of $S_1$ and $S_2$ are defined with bounds $U_1$ and $U_2$, respectively.
2. Apply the $\mu$ analysis using a gain-based method.
   a) Initialize the algorithm with two guessed gains $W_L$ and $W_H$ for $\mu$ peaks below and over 1, respectively,
   b) **while** $|W_H - W_L| > \varepsilon$, where $\varepsilon$ is a user-defined threshold.
      i. Compute an averaged value $W_M$ of $W_L$ and $W_H$ at each iteration
      ii. **if** the corresponding $\mu_{\text{peak}} < 1$.
      iii. Let $W_L = W_M$,
      iv. **else**
      v. Let $W_H = W_M$.
      vi. **end**
      vii. Increase the number of iterations by 1.
   c) **end**
   d) Return the worst-case parameter values $X_{1,\text{wc}}$ and the redefined bounds $U_{1,\text{wc}}$ for $S_1$.
3. Choose the desired optimization algorithm between DIRECT and DE and apply the optimization-based VV,
   a) **if** DIRECT is selected.
      i. Set $S_1$ as known uncertain parameters with fixed values $X_1 = X_{1,\text{wc}}$.
      ii. Initialize $S_2$ with random candidate solution and bounds $U_2$.
      iii. Apply DIRECT for a fixed number of iterations.
      iv. Return the solution for $S_2$,
   b) **else**
      i. Initialize $S_1$ with $X_{1,\text{wc}}$ and bounds $U_1 = U_{1,\text{wc}}$ and $S_2$ with random candidate and bounds $U_2$.
      ii. Apply DE for a fixed number of iterations.
      iii. Return the solution for $S$ (for local algorithm Nelder–Mead, the same procedure can be used as for DE.)
   c) **end**



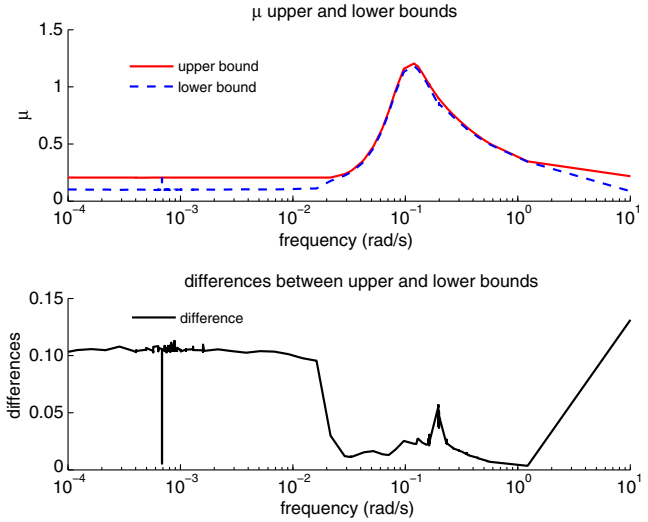


**Fig. 2 Robust performance analysis results.**

the full terminal phase. The $\mu$ analysis is performed on the LFT model of the uncertain six degree of freedom rendezvous system, and the results are given in Fig. 2. The top graph shows the upper bound and lower bound of $\mu$ with a peak value around 1.2. The bottom graph presents the difference between the lower bound and upper bound of $\mu$ to provide a measurement of confidence in the computed $\mu$ value: closer bounds implicate a better knowledge of the true $\mu$ value. For the region of interest around the peak, around 0.1 rad/s, this difference is below 0.05, and hence the peak value of $\mu$ is well characterized by its bounds at the frequency of the worst case. The results obtained are then used to derive the redefined search region together with the initial search point as explained in Sec. III. The upper bound and lower bound peaks, which define the gauranteed performance region and worst case, are subsequently used to define the scattering area for the LFT parameters in optimization approaches as discussed in [8,9]. In addition, the initial conditions and thruster misalignment, which are not taken into account directly in the LFT, are uniformly scattered.

Since the time domain simulation of the full terminal phase scenario is computationally expensive (each simulation takes almost 40 min), a fixed termination strategy is used for the optimization algorithms. Thus, the optimization is stopped after a predefined number of simulations. As shown in Table 1, using this approach, the local Nelder–Mead simplex algorithm can find the worst case very fast within the modified search domain, with only 17 simulations required to get the first violation of the criterion, while 20 out of 200 cases are found to be unsuccessful.

For the population-based algorithm DE, using 150 simulations, 21 of them were found to be unsuccessful after removing the repeated cases between different iterations. The DIRECT algorithm converged more slowly when the dimension of the search space was high. In this case, the size of the uncertainty set was reduced by setting some uncertain parameters at their worst-case points found via $\mu$. Through this strategy, the results show that the DIRECT algorithm can quickly identify the first violation of the figure of merit at only the seventh simulation, while overall 12 out of 150 cases are found to be unsuccessful. The relative trajectories of the chaser during the approach are shown in Fig. 3 for the worst cases found by the local, DE, and DIRECT methods, respectively. 1000 Monte Carlo simulation runs identified only seven occurrences of violation, of which the first violation occurred at the 65th simulation. Moreover, the cost driven optimization $\mu$/DE reached a cost value 4.3 times higher than the Monte Carlo with 15% of the simulation runs. Considering that 1000 runs takes 10–12 days to complete, it is clear that the demonstrated efficiency of these methods with respect to Monte Carlo results in striking computational savings. It can be seen that, although for all cases the hopping phases were performed successfully, the final locations are far from the reference capture point. These capture

**Table 1 Worst-case results using different integrated methods**

| Method | $E_{\text{wc}}$, % | $E(Xl_f)$, % | $E(Vl_f)$, % | $E(V\text{lon}_f)$, % | Simulations | Violations | First violation |
|---|---|---|---|---|---|---|---|
| $\mu$/local | $3.9609 \times 10^4$ | $1.1772 \times 10^5$ | 233.5358 | 872.6166 | 200 | 20 | 17th |
| $\mu$/DE | $1.9598 \times 10^5$ | $5.8283 \times 10^5$ | $4.9734 \times 10^3$ | 148.4956 | 150 | 21 | 8th |
| $\mu$/DIRECT | $1.3803 \times 10^5$ | $4.0397 \times 10^5$ | $6.5079 \times 10^3$ | $3.6085 \times 10^3$ | 150 | 12 | 7th |
| MC | $4.5508 \times 10^4$ | $1.3402 \times 10^5$ | $1.9981 \times 10^3$ | $5.0784 \times 10^2$ | 1000 | 7 | 65th |

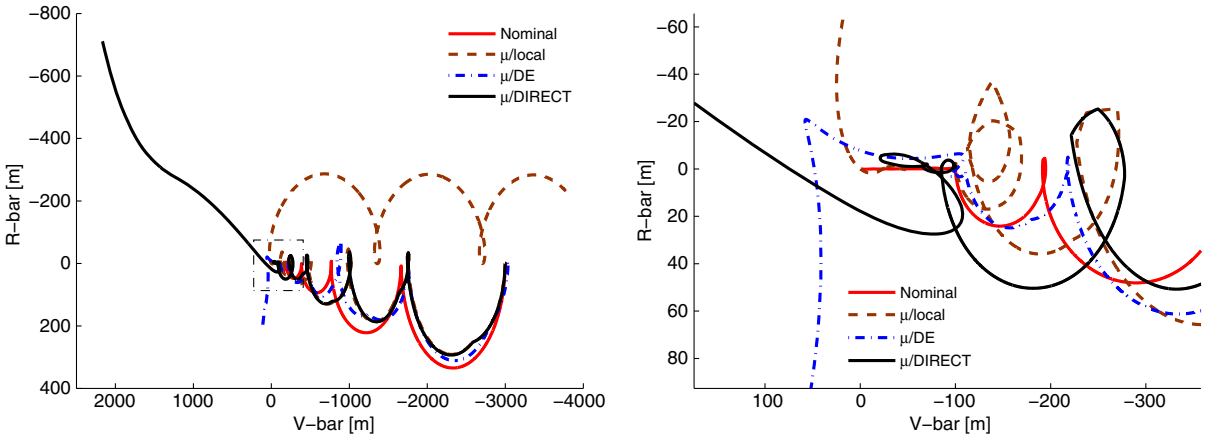


**Fig. 3 Worst-case relative trajectories using $\mu$/local, $\mu$/DE, and $\mu$/DIRECT are compared with the nominal.**

failures are due to the GNC system being unable to start the forced motion or keep the system under control during the forced motion.

## V. Conclusions

Two completely different approaches to VV, i.e., linear frequency-domain $\mu$ analysis and nonlinear time-domain optimization-based worst-case analysis, have been combined into an integrated VV framework in this paper and have been successfully applied to the industrial standard autonomous rendezvous simulator. A major advantage of the proposed integrated VV approach is that initial points and regions in parameter space that are identified by the linear frequency domain tools such as $\mu$ analysis can be used to significantly improve the performance and convergence rate of the optimization-based worst-case search. Three different strategies have been proposed for integrating analytical and optimization-based methods, and these strategies have shown to provide significant computational savings.

## Acknowledgment

This work was funded by the European Space Agency (ESA) under contract 21629/08/NL/EK.

## References

[1] Fehse, W., *Automated Rendezvous and Docking of Spacecraft*, Cambridge Univ. Press, Cambridge, England, U.K., 2003, pp. 362–423.

[2] Kawano, I., Mokuno, M., Kasai, T., and Suzuki, T., "Result and Evaluation of Autonomous Rendezvous Docking Experiments of ETS-VII," *Proceedings of the AIAA Guidance, Navigation and Control Conference*, AIAA Paper 1999-4073, Aug. 1999.

[3] Bateman, A., Balas, G. J., Cooper, J., Aiello, M., and Ward, D., "Analytical and Simulation-Based Control Law Robustness Validation Using CEASAR," *Proceedings of the AIAA Guidance, Navigation and Control Conference*, AIAA Paper 2008-6655, Aug. 2008.

[4] Polites, M. E., "Technology of Automated Rendezvous and Capture in Space," *Journal of Spacecraft and Rockets*, Vol. 36, No. 2, 1999, pp. 280–291. doi:10.2514/2.3443

[5] Menon, P. P., Postlethwaite, I., Marcos, A., Bennani, S., and Bates, D. G., "Robustness Analysis of a Reusable Launch Vehicle Flight Control Law," *Control Engineering Practice*, Vol. 17, No. 7, 2009, pp. 751–765. doi:10.1016/j.conengprac.2008.12.002

[6] Nelder, J. A., and Mead, R., "A Simplex Method for Function Minimization," *Computer Journal*, Vol. 7, No. 4, 1965, pp. 308–313. doi:10.1093/comjnl/7.4.308

[7] Strippoli, L., Colmenarejo, P., Modrego, D., Peters, T. V., Le Peuvédic, C., Guiotto, A., and Salehi, S., "Advanced GNC Solutions for Rendezvous in Earth and Planetary Exploration Scenarios," *59th International Astronautical Congress* IAC-08.A3.I.15, Glasgow, Scotland, 2008, pp. 1793–1807.

[8] Kron, A., Hamel, J. F., Garus, A., and De Lafontaine, J., "$\mu$-Analysis Based Verification and Validation of Autonomous Satellite Rendezvous Systems," *Proceedings of the 18th International Federation of Automatic Control (IFAC) Symposium on Automatic Control in Aerospace*, Nara-ken Shinkokaido, Japan, Sept. 2010, pp. 327–332. doi:10.3182/20100906-5-JP-2022.00056

[9] Kron, A., Bilodeau, V. S., and Ankersen, F., "Enhanced Linear Fractional Transformation: A Matlab Toolbox for Space System Modelling and Controller Analysis and Synthesis," *Proceedings of the 19th International Federation of Automatic Control (IFAC) Symposium on Automatic Control in Aerospace*, Univ. of Wurzburg, Wurzburg, Germany, Sept. 2013, pp. 512–517. doi:10.3182/20130902-5-DE-2040.00136

[10] Wang, W., Menon, P. P., Gomes Paulino, N. M., Di Sotto, E., Salehi, S., and Bates, D. G., "Worst-Case Analysis of Autonomous Rendezvous Systems," *Proceedings of the 18th International Federation of Automatic Control (IFAC) Symposium on Automatic Control in Aerospace*, Nara-ken Shinkokaido, Japan, Sept. 2010, pp. 321–326. doi:10.3182/20100906-5-JP-2022.00055

D. Geller
*Associate Editor*